

doi:10.3788/gzxb20184703.0301001

CCD 激光雷达探测白天近地面气溶胶消光系数

孙培育^{1,2}, 苑克娥¹, 杨杰^{1,3}, 胡顺星¹

(1 中国科学院安徽光学精密机械研究所 中国科学院大气光学重点实验室, 合肥 230031)

(2 中国科学院大学, 北京 100049)

(3 中国科学技术大学, 合肥 230026)

摘 要:利用 CCD 激光雷达系统对合肥西郊近地面气溶胶消光系数进行了昼夜连续测量, 弥补了传统后向散射激光雷达近地面盲区 and 重叠区域的数据空白, 比较夜间 Mie 散射气溶胶激光雷达和 CCD 激光雷达获得的气溶胶消光系数, 验证了 CCD 激光雷达系统的可靠性. CCD 激光雷达系统的白天检测是可行的, 并获得了 10~180 m 高度的大气气溶胶消光系数, 空间分辨率最高可达 1 cm. 两种气溶胶消光系数分布表明, 气溶胶消光系数在垂直方向上不是单调递减, 且在一天中剧烈变化. CCD 激光雷达检测到的气溶胶消光系数的时空演化图表明, 随着天色变黑, 整体气溶胶具有降低的趋势. CCD 激光雷达的气溶胶消光系数曲线的日间检测是可以实现的.

关键词:大气光学; 气溶胶探测; CCD 激光雷达; 白天探测; 消光系数

中图分类号: P412.291

文献标识码: A

文章编号: 1004-4213(2018)03-0301001-7

Measurement of Extinction Coefficient of Near-surface Aerosol by CCD Lidar in the Daytime

SUN Pei-yu^{1,2}, YUAN Ke-e¹, YANG Jie^{1,3}, HU Shun-xing¹

(1 Key Laboratory of Atmospheric Optics, Anhui Institute of Optics and Fine Mechanics, Chinese Academy of Sciences, Hefei 230031, China)

(2 University of Chinese Academy of Sciences, Beijing 100049, China)

(3 University of Science and Technology of China, Hefei 230026, China)

Abstract: Atmospheric aerosol extinction coefficient vertical profiles of near-surface in Hefei western suburb were measured by a CCD lidar system in the day and night, which could fill the gap of the traditional Mie-scattering lidar system especially in the blind area and overlapped region. By comparison of the aerosol extinction coefficient retrieved by Mie-scattering aerosol lidar and CCD lidar at night, the reliability of the CCD lidar system was verified, and the daytime detection of the CCD lidar system was feasible. Profiles of atmospheric aerosol extinction coefficient for 10-180 m altitude were obtained with high spatial resolution, of which the highest resolution was up to 1 cm. Two cases of aerosol extinction coefficient profiles showed that the aerosol extinction coefficient was not monotone decreasing in vertical direction, at the same time, changed violently in the day. The spatio-temporal evolution of aerosol extinction coefficient retrieved by CCD lidar showed that the overall aerosol had a tendency to reduce as

Foundation item: The National Natural Science Foundation of China (No. 41475001)

First author: SUN Pei-yu (1991—), male, Ph.D. degree candidate, mainly focuses on atmospheric measurement of lidar system. Email: spy19910609@126.com

Supervisor: HU Shun-xing (1966—), male, professor, Ph.D. degree, mainly focuses on atmospheric measurement methodology and technology with diverse lidar systems. Email: sxhu@aiofm.ac.cn

Corresponding author: YUAN Ke-e (1978—), female, professor, Ph.D. degree, mainly focuses on atmospheric measurement of lidar system. Email: keyuan@aiofm.ac.cn

Received: Sep.29, 2017; **Accepted:** Nov.20, 2017

<http://www.photon.ac.cn>

the day getting dark. The daytime detection of aerosol extinction coefficient profile by using CCD lidar is credible and fulfilled.

Key words: Atmospheric optics; Aerosol detection; CCD lidar; Daytime detection; Extinction Coefficient

OCIS Codes: 010.1100; 010.3640; 040.1520; 290.1310

0 Introduction

Atmospheric aerosol is a heterogeneous system composed of solid and liquid particles suspended in the atmosphere. The diameter of atmospheric aerosol particle is generally between 10^{-3} and 10^2 μm . Many processes can produce aerosols, which fall into two major categories according to their sources, natural aerosols and human aerosols. Natural aerosol sources are mainly from oceans, soil and biosphere and volcanoes, etc^[1]; Human aerosol sources are mainly from combustion of fossil fuels, industrial and agricultural production activities, and automobile exhaust and so on. Although aerosols are only a small fraction of the content of the earth's atmosphere, they are increasingly valued due to their important role in many atmospheric processes.

The radiation effect of aerosol affects the radiation balance of the ground-gas system, which causes climate change. The aerosols close to the ground are closely related to human health. As China is in the stage of rapid economic development, industrial pollution is becoming more and more serious. In recent years, atmospheric aerosol particles have increased significantly, so the detection of the aerosol distribution is of great significance^[2-4].

Atmospheric aerosol extinction coefficient is an important physical parameter in research on atmospheric laser transmission, and the near-surface aerosol data with high spatial resolution is less. On one hand, the direct detection equipment does not have the spatial resolution^[5-6]; on the other hand, the detection range of traditional back-scattering lidar is generally above a few kilometers, while in the near distance due to its own blind area and the geometrical factor correction error, there is no valid data^[7-9]. The CCD lidar system adopts a lateral camera, which is a perfect solution to the blind area problem of traditional back-scattering lidar system. There is no geometric factor correction problem using CCD lidar system, which provides a strong support to making up for near-surface atmospheric aerosol data. The CCD lidar system has already been used for horizontal measurements by Liu Xiaoqin and her group^[10]. And Ma Xiaomin and her group used the CCD lidar system for vertical measurements only at night^[11]. Now we use it to measure aerosol extinction coefficient vertically in the daytime, of which the retrieval method is different and the signal extraction is difficult.

1 CCD Lidar System

The CCD lidar system uses the CCD camera equipped with cradle head to collect the aerosol scattering signal from the lateral side^[12]. It is simple, portable, cheap and practical, which is set up by our research team. As shown in Fig.1, the CCD lidar system is mainly divided into three parts: the laser transmitting system, the receiving system and the data processing system.

The transmitting system is a high-frequency semi-conductor solid-state laser with a pulse repetition frequency from 10 kHz to 100 kHz. The model is Sol 3 W-5 W-10 W 532 with an emission wavelength of 532 nm. The beam diameter is less

than 8 mm, so the energy is concentrated, which is benefitted for observation during the day. The operating temperature is $15\sim 40$ $^{\circ}\text{C}$, which is limited to the working environment neither too hot nor too cold. The laser is supported by a self-made iron frame to ensure the laser light vertical to the ground.

The receiving system is composed of industrial CCD camera, filters, fixed focus lens, cradle head and

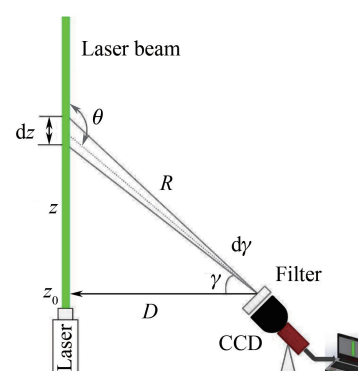


Fig.1 Diagram of CCD lidar system

tripod. The model of the industrial CCD camera is Manta 201b, whose pixels are $1\ 624(\text{H}) \times 1\ 234(\text{V})$, each pixel's size is $4.4\ \mu\text{m} \times 4.4\ \mu\text{m}$. Because the lens mount of the CCD is C-mount, and the Nikon digital lens is F-mount, an adapter ring is used to connect both. The focal length of the Nikon digital lens is 16 mm. Several filters had been used for experiment; it is found that the filter with a bandwidth of 0.5 nm at 532 nm is suitable for daytime detection. If the bandwidth is too narrow, the beam light may be filtered out. If the bandwidth is too wide, the background noise is too strong. The cradle head produced by Shandong Wanteng Company can accurately adjust the pitch angle with the accuracy of $\pm 0.01^\circ$, which is necessary to confirm the altitude. The detailed parameters of the CCD lidar system are shown in Table 1.

Table 1 Specifications of CCD Lidar System

Lasers	Sol 3 W-5 W-10 W
Wavelength	532 nm
Output power	>10 W
Q-switch repetition rate	10 kHz to 100 kHz
Pulse width	7 to 50 ns
Beam diameter	<8 mm
Electrical requirements	24 V DC/16 A
Operating temperature	15-40 °C
Detector	Manta G201b
Pixels	1 624(H) × 1 234(V)
Pixel size	4.4 μm × 4.4 μm
Lens mount	C-Mount
ADC	12 bit
Lens focal length	16 mm
Filter bandwidth	0.5 nm

The data processing system is a Lenovo notebook computer, which needs to support the USB 3.0 interface. The images with the background preliminarily deducted are read into Matlab, after data extraction, data stack, moving average and a series of treatments, the atmospheric aerosol extinction coefficient profiles are obtained.

2 Retrieval principle of aerosol extinction coefficient for CCD lidar

Received by a pixel with field of view from a distance z , the power E_1 , located at the angle of θ and the angle range of $d\theta$ (corresponding to the length dz) satisfies the following lidar equation^[13]

$$E_1 = K_1 \beta(z, \theta) T_z T_r \quad (1)$$

where, K_1 is the constant of CCD lidar system including a CCD lens area, a laser emitting energy and an optical efficiency, etc. $\beta(z, \theta)$ is the angle scattering coefficient of the atmospheric particle at a height z and a scattering angle θ . T_z denotes the transmittance in the direction of z . T_r represents the transmittance in the direction of r .

The extinction coefficient is expressed as the sum of the scattering coefficient and the absorption coefficient. Taking into account that the urban atmospheric aerosol absorption coefficient is relatively small, the extinction coefficient referred to in this article means the total scattering coefficient of aerosols without special illustration.

$$\sigma = \int_{4\pi} \beta(\theta) d\Omega \quad (2)$$

In order to show the change of the scattered light intensity with the scattering angle θ , the ratio of the angular scattering cross section $\beta(\theta)$ in the direction of the angle θ to the mean value of all the angular scattering cross sections $\beta_s/4\pi$ is defined as the scattering phase function $P(\theta)$

$$P(\theta) = \frac{\beta(\theta)}{\beta_s/4\pi} \quad (3)$$

The scattering phase function $P(\theta)$ reflects the spatial distribution of the scattering intensity of aerosol particles, including the aerosol particle shape, particle size, refractive index and other information. Substituting Eq. (2) and Eq.(3) into Eq.(1), we can obtain

$$E_1 = K_2 T_z T_r \sigma_s(z) P(\theta) \quad (4)$$

The K_2 is constant. The scattering phase function $P(\theta)$, which is contained in the formula, is currently calculated by using the HG model as following

$$P_{HG}(\theta, g) = \frac{1}{4\pi} \cdot \frac{1 - g^2}{(1 + g^2 - 2g \cos \theta)^{3/2}} \quad (5)$$

Based on the above Eq. (1) to Eq. (5), we can get the formula for detecting the aerosol extinction coefficient profile by means of a CCD lateral scattering lidar.

$$\begin{cases} E_1(\theta) = K_2 T_z T_r \sigma_s(\theta) P_{HG}(\theta, g) \\ T_z T_r = \exp \left[- \int_0^z \sigma(z) dz - \int_0^r \sigma^*(r) dr \right] \\ \sigma_{aer} = \sigma_s - \sigma_{atm} \end{cases} \quad (6)$$

In the formula, $E_1(\theta)$ stands for the lateral scattering signal intensity, that is the gray value. $T_z T_r$ is the atmospheric transmittance of the emission path and the reception path, $\sigma(z)$ and $\sigma^*(r)$ are the extinction coefficient at the height of z and the slant path of r , respectively. σ_{aer} , σ_{atm} , σ_s represent the extinction coefficient of the aerosol, the molecule and the total, respectively. The inversion Eq. (6) can be considered as a recursive relation

$$\begin{cases} \sigma_s(\theta_1) = \frac{E_1(\theta_1)}{P_{HG}(\theta_1) K_2 \exp[-D\sigma_s(\theta_1)]} & n = 1 \\ \sigma_s(\theta_{n+1}) = \frac{E_1(\theta_{n+1})}{P_{HG}(\theta_{n+1}) K_2 T_z(\theta_n) T_r(\theta_n)} & n > 1 \end{cases} \quad (7)$$

The extinction coefficient value of the $n+1$ th point can be obtained by substituting the transmittance obtained from the previous n points into the recursive formula. The extinction coefficient changes with the scattering angle θ . The scattering angle θ and the altitude z have a one-to-one correspondence. Then we can get the vertical profile of the atmospheric aerosol extinction coefficient.

3 The way to realize daytime measurement

As we all know, the daytime measurement of CCD lidar system is influenced by the strong solar background. To overcome this problem, several ways have been improved as follows. Firstly, the camera lens with a small angle of field of view is used, and a filter with a narrow bandwidth of 0.5 nm at 532 nm is located between the lens and the CCD camera. Secondly, the exposure time is short, less than 1 s. Data averaging and data smoothing technique efficiently improve the ratio of signal to noise so as to reduce the influence of solar background light. Thirdly, the laser power increases, so the effective echo signal is also very strong. At last, a new background subtraction method and the Gauss fitting method are adopted to extract the light column, at the same time, the wavelet transform is used to smooth the noise, which greatly improves the signal-to-noise ratio.

3.1 Image accumulation average

Shorten the exposure time can effectively reduce the background light from the sun. However, the other noises are fixed, such as dark current noise and so on, which will reduce the signal to noise ratio. Based on the error theory, we know that cumulative average can decrease the random error. From the Fig. 2, we can see that the signal-to-noise ratio of fifty times cumulative average is better than that of once. The more images are stacked, the better the signal-to-noise ratio. When a certain number of accumulated value is reached, the speed of increase of SNR begins to decrease rapidly, at the same time, the speed of computer processing will also slow down. So we usually superimpose 50 or 100 images in the experiment.

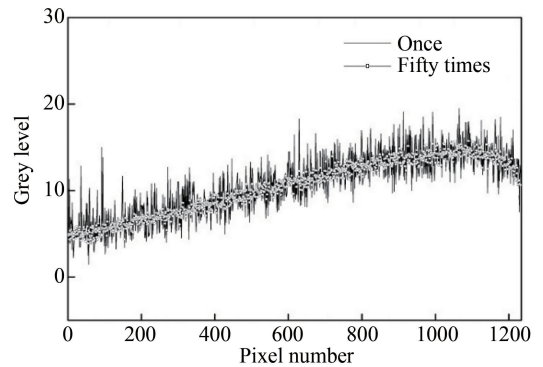


Fig.2 Signal curves of fifty times cumulative average and once

3.2 The Gauss fitting method

The monochromaticity of the high-frequency laser is very good, and its scattered light generated by interaction with atmospheric molecules and aerosols meet the Gaussian distribution. The signal of scattered light takes up several pixels on each corresponding row of the image. The relationship between the total number of photons N and the pixel position coordinate x can be expressed as

$$N_{\text{total}}(x) = A_0 \exp[-(x - A_1)^2 / (2A_2^2)] + A_3 \quad (8)$$

In the formula, the range of x is the transverse width of the capture images. A_0 is the peak height of the Gaussian curve, A_1 is the center position coordinate of the beam, A_2 is the standard deviation of the Gaussian fit, and A_3 is the remains of background noise. The laser scattering echo intensity N_s corresponding to each pixel in the direction of the beam can be expressed by the net area of the Gaussian fit curve corresponding to that pixel:

$$N_s = \sqrt{2\pi} A_0 A_2 \quad (9)$$

The images with the background preliminarily deducted are read into Matlab, and the Gaussian fitting of the above formula is applied to each row of the image using Matlab programming. Then, according to the parameters after fitting, the corresponding laser scattering echo intensity N_s can be obtained, which is related to the $E(\theta)$. The three-dimensional Gaussian fit of the scattered echo intensity is shown in Fig. 3.

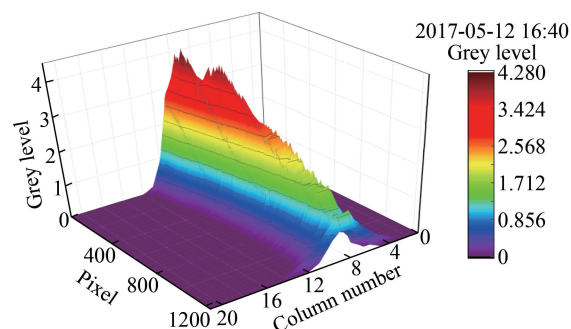


Fig.3 Three-dimensional Gaussian fit of the scattered echo intensity

3.3 Correction of pixel angle

Because the precision of hardware manufacturing, each pixel angle of the CCD camera exists the error. In order to correct the error, we design an experiment using the checkerboard. The schematic diagram is as follows.

Through some geometric calculation, the distribution of each pixel angle is obtained. As shown in the Fig. 5, the overall pixel angle changes little. In the pixel number of about 1 200, there is a decline slope. When retrieving the aerosol profile, the pixel angle is from the correction curve in the Fig 5.

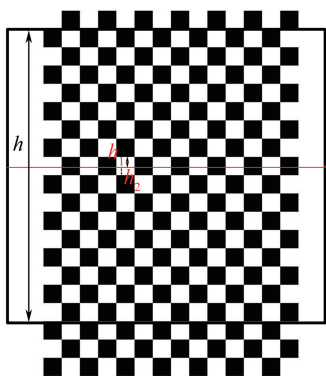


Fig.4 Schematic diagram of measuring pixel angle

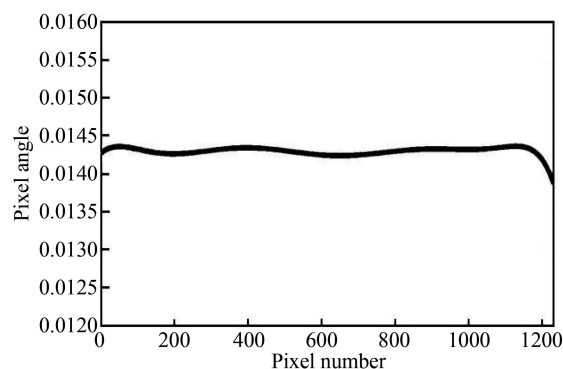


Fig.5 Distribution of each pixel angle

4 Daytime detection of CCD lidar system

4.1 Comparison analysis of daytime data

In order to verify the reliability of the aerosol extinction coefficient of the CCD lidar system, the aerosol extinction coefficient retrieved by Mie-scattering aerosol lidar, whose technology is more mature, is used for comparison. The spatial resolution of the Mie lidar is 7.5 m, and the time resolution is 10 min. The inversion method is the relatively mature Fernald recursive method^[14], which is retrieved from the high altitude. The comparison results are shown in Fig. 6, in which the dotted line represents the aerosol extinction coefficient profile retrieved by Mie lidar, the solid line stands for the aerosol extinction coefficient profile retrieved by CCD lidar. In order to make the result real, the original Mie lidar

data is used for comparison without geometric factor correction. It can be seen from the dotted line that the extinction coefficient of aerosol reaches the maximum at about 1 km, and then the extinction coefficient of aerosol decreases gradually as altitude increases to the overall trend, which means that the blind area and overlapped region of this Mie-scattering lidar system is about 1 km. It can be seen from the solid line that the extinction coefficient of aerosol retrieved by CCD lidar decreases slowly from the near ground to about 1 km, then decrease quickly above 1 km. However, the resolution of CCD lidar system is poor above 1.5 km, which doesn't demonstrate the details from 1.5 km to 2 km.

It can be seen that in the range of 1 km~1.5 km, the aerosol extinction coefficient profiles retrieved by the two lidar systems match well, of which the average relative error is less than 15%. Because the two lidar systems are about 100 meters horizontally apart, and there is a southeast wind with wind speed of about 1 m/s, the aerosol horizontal distribution is not uniform, so their inversions of aerosol extinction coefficient are slightly different. As the CCD camera has a photometric sensitivity threshold, the distant scattering echo is too weak to be able to image on the CCD camera, even if it can be photographed at the top of the sky. It can be seen from Fig. 2 that the aerosol extinction coefficient of the CCD lidar reduce rapidly at 1.4 km or more, because the echo signal received by the CCD camera is close to the CCD camera's own photometric threshold. Therefore, the echo signal is no longer accurate, and the aerosol extinction coefficient retrieved is also not accurate. The advantage of the CCD lidar system is the high resolution in the near distance, and the disadvantage of which is the poor resolution in the far distance. So the maximum detection height of this CCD lidar system is about 1.4 km at night, the maximum detection of this CCD lidar system in the daytime is depended on the effect of filter, the intensity of background and so on.

4.2 Spatio-temporal evolution of aerosol extinction coefficient

Fig. 7 is the spatio-temporal evolution of aerosol extinction coefficient retrieved by CCD lidar from 16 o'clock to 20 o'clock. From Fig. 7, it can be seen that as the sky got dark, the overall aerosol had a tendency to reduce. The reason was that the aerosol close to the ground was mainly produced by human activity, as the sky getting darker, the human activity becoming weaker. At 16:00, there was a peak of aerosol extinction coefficient at the altitude of about 80 m, while at 16:30, the peak of aerosol extinction coefficient moved to the altitude of about 45 m. This might be related to factors such as uneven temperature, heat convection, and atmospheric turbulence, etc. Since the atmospheric turbulence was more active in the afternoon than that in the evening, the aerosol extinction coefficient changed violently before 17 o'clock. How these factors affect the aerosol extinction coefficient needs for further research.

5 Conclusion

A CCD lidar system was used to measure the atmospheric aerosol extinction coefficient profiles of near-surface in Hefei western suburb by imaging the laser beam from the lateral side both in the day and

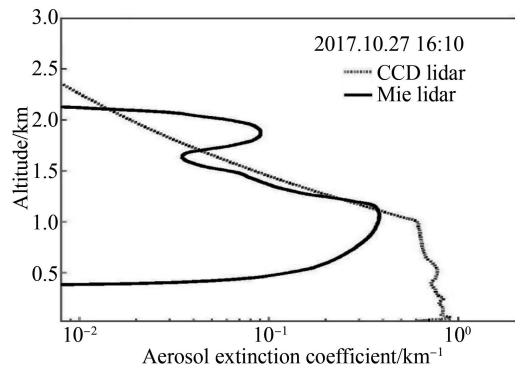


Fig.6 Comparison of aerosol extinction coefficient profiles from Mie lidar and CCD lidar at 16:10 on October 27, 2017

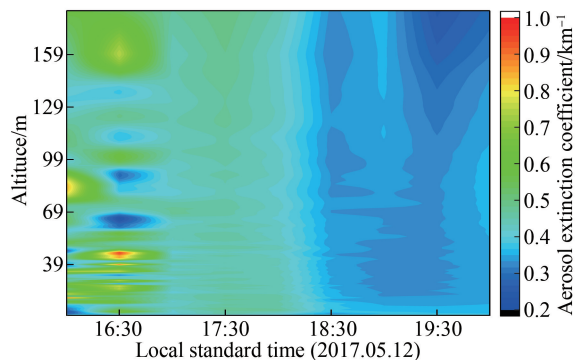


Fig. 7 Spatio-temporal evolution of aerosol extinction coefficient retrieved by CCD lidar

night. Firstly, the structure diagram of the CCD lidar system was demonstrated, the parameters of which were listed. Then, the principle of the CCD lidar system was introduced, and the inversion formulas were derived. By comparison of the aerosol extinction coefficient retrieved by Mie-scattering aerosol lidar and CCD lidar at night, the reliability of the CCD lidar system was verified, and the daytime detection of the CCD lidar system was feasible. Two cases of aerosol extinction coefficient profiles showed that the aerosol extinction coefficient was not monotone decreasing in vertical direction, at the same time, changed violently in the day. The spatio-temporal evolution of aerosol extinction coefficient retrieved by CCD lidar showed that the overall aerosol had a tendency to reduce as the day getting dark.

In a word, the CCD lidar system can well make up for the gap of the traditional back-scattering Mie-lidar system near surface. At present, this CCD lidar system can only experiment on condition that the sun is not very strong in the daytime. The next step is to improve the equipment, including filters, CCD camera and so on. And then, the continuous aerosol extinction coefficient profiles under strong background condition can be obtained, at the same time; the maximum detection height in the daytime will be improved.

References

- [1] YAMAMOTO G, TANAKA M. Increase of global albedo due to air pollution[J]. *Journal of Atmospheric Sciences*, 1972, **29**(1): 1405-1412.
- [2] BARNES J E, BRONNER S, BECK R, et al. Boundary layer scattering measurements with a charge-coupled device camera lidar[J]. *Applied Optics*, 2003, **42**(15): 2647-2652.
- [3] BARNES J E, HOFMANN D J. Variability in the stratospheric background aerosol over Mauna Loa Observatory[J]. *Geophysical Research Letters*, 2001, **28**(15): 2895-2898.
- [4] BARNES J E, SHARMA N C, KAPLAN T B. Atmospheric aerosol profiling with a bistatic imaging lidar system[J]. *Applied Optics*, 2007, **46**(15): 2922-2929.
- [5] BARNES J E, SHARMA N C P. An inexpensive active optical remote sensing instrument for assessing aerosol distributions[J]. *Journal of the Air & Waste Management Association*, 2012, **62**(2): 198-203.
- [6] LIN Jin-ming, MISHIMA H, KAWAHARA T D, et al. Bistatic imaging lidar measurements of aerosols, fogs, and clouds in the lower atmosphere[C]. SPIE, 1998, **3504**: 550-557.
- [7] MEKI K, YAMAGUCHI K, LI X, et al. Range-resolved bistatic imaging lidar for the measurement of the lower atmosphere[J]. *Optics Letters*, 1996, **21**(17): 1318-1320.
- [8] REAGAN J A, BYRNE D M, HERMAN B M. Bistatic LIDAR: A tool for characterizing atmospheric particulates: part i---the remote sensing problem[J]. *IEEE Transactions on Geoscience & Remote Sensing*, 1982, **20**(3): 229-235.
- [9] REAGAN J A, BYRNE D M, HERMAN B M. Bistatic LIDAR: A tool for characterizing atmospheric particulates: part ii---the inverse problem[J]. *IEEE Transactions on Geoscience & Remote Sensing*, 2007, **45**(3): 236-243.
- [10] LIU Xiao-qin, HOU Zai-hong, QIN Lai-an, et al. A portable imaging lidar for lower boundary layer atmospheric measurement[C]. SPIE, 2015: 96450R.
- [11] MA Xiao-min, ZHANG Hui, SHAN Hui-hui, et al. Statistical distribution of aerosol backscattering coefficient profiles in near-ground at west suburb of Hefei in 2014[J]. *Chinese Journal of Lasers*, 2016, **43**(7): 0705001.
- [12] PARAMESWARAN K, ROSE K O, MURTHY B V K. Aerosol characteristics from bistatic lidar observations[J]. *Journal of Geophysical Research Atmospheres*, 1984, **89**(D2): 2541-2552.
- [13] MENG Xiang-qian, HU Shun-xing, WANG Ying-jian, et al. Aerosol scattering phase function and visibility based on charge coupled device[J]. *Acta Optica Sinica*, 2012, **32**(9): 8-13.
- [14] FERNALD F G. Analysis of atmospheric lidar observations: some comments[J]. *Applied Optics*, 1984, **23**(5): 652-653.